Viral Evolution under the Pressure of an Adaptive Immune System: Optimal Mutation Rates for Viral Escape

CHRISTEL KAMP,[1] CLAUS O. WILKE,[2] CHRISTOPH ADAMI,[2,3] AND STEFAN BORNHOLDT[1,4]

[1]*Institut für Theoretische Physik und Astrophysik, Universität Kiel, Leibnizstrasse 15, 24098 Kiel, Germany*

[2]*Digital Life Laboratory 136-93, California Institute of Technology, Pasadena, California 91125*

[3]*Jet Propulsion Laboratory 126-347, California Institute of Technology, Pasadena, California 91109*

[4]*Interdisziplinäres Zentrum für Bioinformatik, Universität Leipzig, Kreuzstrasse 7b, 04103, Leipzig, Germany*

Received August 28, 2002; revised October 28, 2002; accepted October 28, 2002

Based on a recent model of evolving viruses competing with an adapting immune system (Kamp and Bornholdt, Co-evolution of quasispecies: B-cell mutation rates maximize viral error catastrophes. Phys Rev Lett 88, 2002), we study the conditions under which a viral quasispecies can maximize its growth rate. We find that a virus is most viable if it generates on average precisely one mutation within the time it takes for the immune system to adapt to a new viral epitope. Experimental viral mutation rates, in particular for HIV (human immunodeficiency virus), seem to suggest that many viruses have achieved their optimal mutation rate. © *2003 Wiley Periodicals, Inc.*

Key Words: quasispecies; co-evolution; virus mutation rate; adaptive immune system; HIV

1. INTRODUCTION

Since Eigen and Schuster introduced the concept of a quasispecies [1, 2], it has become a standard model to describe molecular and viral evolution. If a simple, single-peaked fitness landscape is assumed, quasispecies theory predicts that error-prone replication leads to the formation of a central "master sequence," surrounded by a cloud of mutant sequences. For viral evolution, this implies that any "wild-type" sequence is accompanied by a cloud of related mutants that, as a whole, represent a target for the immune system. The quasispecies approach to molecular evolution has been the object of detailed investigations, often supported by techniques of statistical physics [3–14], revealing the characteristic features of such systems, including the occurrence of an error catastrophe. The latter characterizes a system in which a critical mutation rate exists beyond which the genomic information is irretrievably lost to mutations, i.e., beyond which selection ceases to operate [10–12, 15–18] (for an in-depth discussion of error catastro-

Correspondence to: Christel Kamp, Blackett Laboratory, Imperial College, Prince Consort Road, London SW7 2BV, United Kingdom; e-mail: c.kamp@imperial.ac.uk

phes and related phenomena see also [19]). The destabilizing effect of increased mutation rates has been observed for various viruses, including HIV [20] and Poliovirus [21].

Recently, various extensions of the Eigen-Schuster model have been considered, in particular involving the shape of the fitness peaks and the landscape's time-dependence. Although the shape of the fitness function influences the robustness of a species to mutations [22–24], a behavior qualitatively different from the standard results can be observed for *nonstationary* fitness landscapes [25, 26]. In rapidly changing environments, a second catastrophe emerges besides the well-known error catastrophe, termed "adaptation catastrophe." In a changing environment, sequence replication must occur with a nonvanishing error rate to enable the species to keep up with the environmental changes. (In static landscapes, a zero mutation rate is ultimately optimal because it maximizes the average global fitness of the population.) Indeed, a selective advantage for so called "mutator mutants" (or "general mutators" [27]) has been observed for *Escherichia coli* and *Salmonella enterica* under challenging living conditions [28–30].

For viruses in the environment of an adaptive immune system, the fitness landscapes for *both* the virus and the immune system are dynamically generated by a co-evolutionary process. These dynamics can be studied within the quasispecies framework if the quasispecies character of both the viral population and the motifs of immune receptors are acknowledged. In an immune response, the presence of an antigenic epitope induces the proliferation of the corresponding immune receptor sequence. This "master" sequence is associated with a cloud of closely related receptor sequences that emerge from somatic hypermutation of B cells in the germinal centers [31]. Competition between a viral population and an adaptive immune system takes place via an asymmetric coupling: although the immune quasispecies is strongly attracted by the virus, the viral quasispecies is driven away from its current master sequence by the immune system. This predator-prey-dynamics results in a migration through sequence space as observed in many infectious diseases, such as HIV [32, 33].

The co-evolutionary dynamics within an infected host was recently formalized within a model relying only on a few dynamical rules [34], recapitulated in the following section. Here, we focus on the implications of an optimal immune response within this framework and consider the conditions that correspond to maximal *viral* fitness. Finally, we compare known viral mutation rates to those expected if a viral population has achieved an optimal mutation rate.

2. VIRUS-IMMUNE SYSTEM CO-EVOLUTION

Let us assume that the viral and the immunological quasispecies alike experience a single-peaked fitness function (Figure 1), albeit one that can change in time. Let us assume further that at any particular time, the (viral) master sequence of length n grows at a rate σ_v (much larger than the "off-peak" or background-fitness η_v), and similarly for the immune system: $\sigma_{is} \gg \eta_{is}$. Such a simple immunological fitness function results from a reduction of the viral impact to induce proliferation of immune cells to its master sequence. Analogously, only the dominant immune sequence imposes a decay rate δ on its complementary viral sequence. Both species replicate imperfectly, with copy fidelities $q_v < 1$ and $q_{is} < 1$ (denoting the probability for correct duplication of a monomer drawn from an alphabet of size λ). The virus-immune system interaction is implemented by the following dynamic rules that are cyclically iterated, leading to the quasispecies' migration through sequence space:

1. Once the immune system imposes a decay rate $\delta > 1$ on the viral master sequence (centered at the viral fitness peak), the narrow niche of the virus is assumed to move to an arbitrary sequence of the first error class (cf. Figure 1, bottom row).
2. The viral quasispecies adapts to this new fitness peak on a time scale τ_v.
3. The fitness peak of the immune quasispecies is adjusted and moves to the new maximum of the viral distribution (cf. Figure 1, top row).
4. The immune system adapts to the new fitness peak on the time scale τ_{is}.

As discussed previously [34], the dynamically generated time scale $\tau = \tau_v + \tau_{is}$ can be approximated by the two expressions:

$$\tau_v \approx -\frac{\ln\left(\frac{1-q_v}{\lambda-1}\right)}{q_v^n(\sigma_v-\eta_v)+\delta} \tag{1}$$

and

$$\tau_{is} \approx -\frac{\ln\left(\frac{1-q_{is}}{\lambda-1}\right)}{q_{is}^n(\sigma_{is}-\eta_{is})}. \tag{2}$$

The relative growth of the (moving) viral and immunological master sequences in comparison to the environmental (background) sequences' growth can be determined as [25, 34]:

$$\kappa_i = \frac{(e^{(q_i^n\sigma_i-\eta_i)\tau} - e^{(q_i^n\eta_i-\eta_i)\tau})(1-q_i)\sigma_i}{(\lambda-1)(\sigma_i-\eta_i)q_i}, \quad i \in \{v,\ is\}, \tag{3}$$

leading to the conditions

FIGURE 1

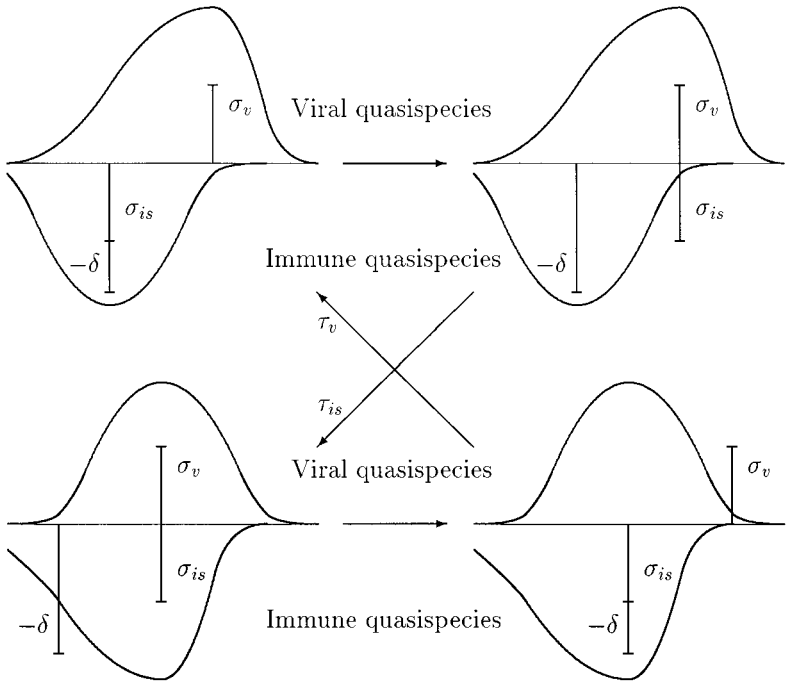

Co-evolution of viral and immune quasispecies. The figure shows the peaked fitness functions (σ_v, σ_{is}) and the decay rate δ locally imposed to the virus by the dominant immune sequence together with the quasispecies evolving in response (distribution of sequences in terms of concentrations).

$$\kappa_v > 1, \qquad \kappa_{is} > 1 \tag{4}$$

for viability of the viral and immunological species, respectively. The regimes of (co)existence of the two quasispecies can be determined by analyzing κ_v and κ_{is}. In particular, the viral quasispecies is subject to both a classical error catastrophe at high mutation rates, and an adaptation catastrophe for small mutation rates. In contrast, the immune system (as the driving force) is not subject to a limiting migration velocity and accordingly only displays the classical error catastrophe [34].

3. OPTIMAL VIRAL MUTATION RATE

Having derived the relations quantifying viral as well as immunological viability, we can now deduce optimal strategies for both the virus and the immune system. The immune system attempts to minimize viral growth ($\partial\kappa_v/\partial q_{is} = 0$), which implies the relation

$$\mu_{is} - 1 - n_{is}\mu_{is}\ln\left(\frac{\mu_{is}}{\lambda - 1}\right) = 0; \quad \mu_{is} = 1 - q_{is} \tag{5}$$

between the optimal immune receptor size n_{is} and the per-site mutation probability μ_{is}. This prediction and how it fares against the background of experimental data has been discussed in Kamp and Bornholdt [34]. Below, we extend this approach to derive the conditions for optimal viral escape from an immune response.

Let us first approximate κ_v in Eq. (3) by

$$\kappa_v \approx \frac{1 - q_v}{\lambda - 1}\exp[(q_v^n\sigma_v - \eta_v)\tau], \tag{6}$$

using $\sigma_v \gg \eta_v$, $q_v \approx 1$. Optimizing viral viability conditions is akin to maximizing the viral species' relative growth rate κ_v such that

$$\frac{\partial\kappa_v}{\partial q_v} = 0. \tag{7}$$

Inserting $\tau = \tau_v + \tau_{is}$ into (6) leads the equivalent condition

$$\begin{aligned} 0 = {} & (q_v^n(\sigma_v - \eta_v) + \delta)(n(q_v - 1)q_v^{2n}\sigma_v^2\tau_{is} \\ & + \delta[q_v + (q_v - 1)nq_v^n\sigma_v\tau_{is}] \\ & + \eta_v[q_v - q_v^{n+1} - (q_v - 1)nq_v^{2n}\sigma_v\tau_{is}]) \\ & + nq_v^n(q_v - 1)(\eta_v^2 - \delta\sigma_v - \eta_v\sigma_v)\ln\left(\frac{1 - q_v}{\lambda - 1}\right). \end{aligned} \tag{8}$$

FIGURE 2

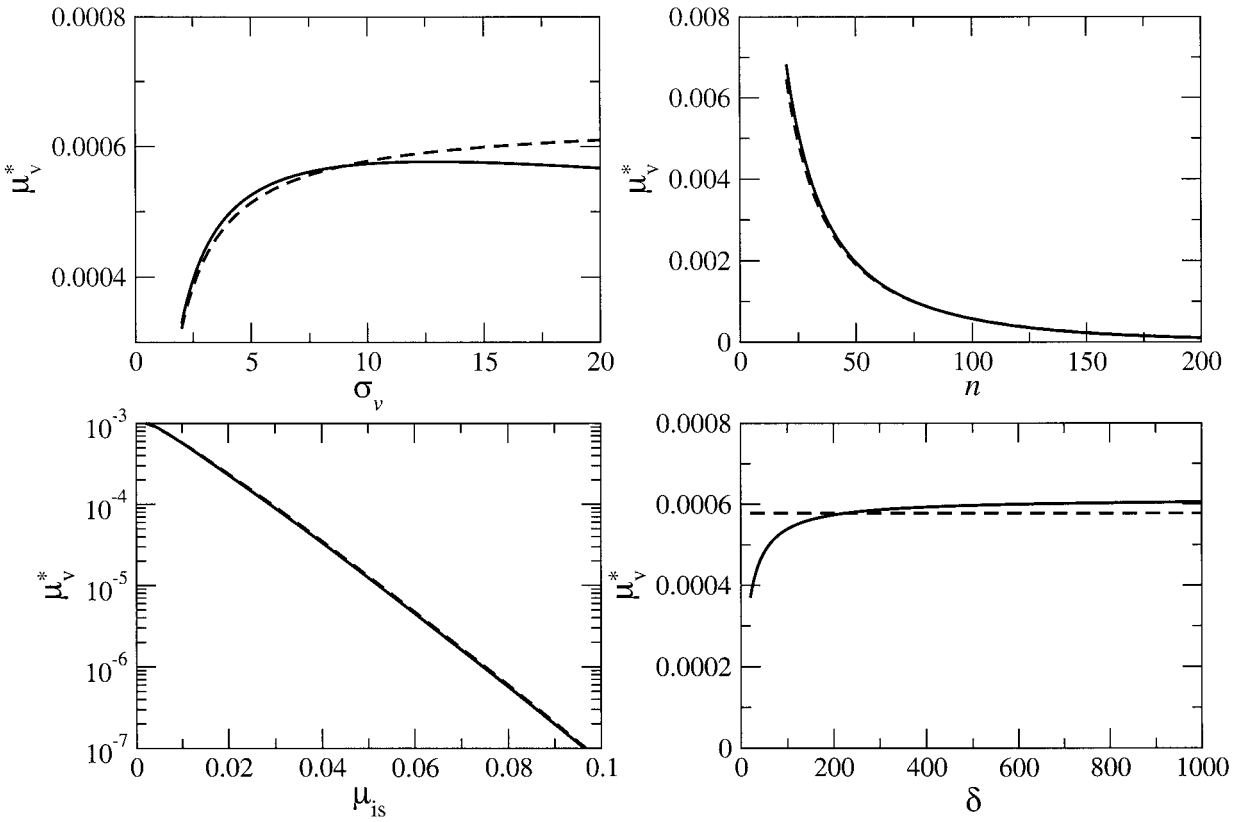

Optimal per-site mutation rate μ^*_ν comparison between the analytic approximation as given by equation (10) (dashed lines) and the numerical solution to equation (7) (solid lines). Parameters are $\sigma_\nu = 10$; $\eta_\nu = 1$; $\sigma_{is} = 10$; $\eta_{is} = 1$; $q = 0.99$; $n = 100$; $\delta = 200$; $\lambda = 4$, unless specified otherwise in the plot.

We can simplify this expression in the following manner. Writing (8) in terms of the mutation probability $\mu_\nu = 1 - q_\nu$, rather than the copy-fidelity q_ν allows us to expand (8) in terms of μ_ν (while leaving the term in $\ln \mu_\nu$ untouched). Assuming furthermore that $\delta \gg \sigma_\nu \gg \eta_\nu$, and $n \gg 1$, we find

$$\frac{\partial \kappa_\nu}{\partial q_\nu} = 0 \Leftrightarrow \delta^2 + n\delta\sigma_\nu(\ln \mu_\nu - \delta\tau_{is})\mu_\nu \approx 0. \qquad (9)$$

We now proceed to determining the root of this expression. Although this can be done numerically (see below), we first attempt to obtain an analytical approximation that permits an intuitive interpretation. For this purpose, it is allowable to assume $\ln \mu_\nu \approx$ const, because $\ln \mu_\nu$ is a slowly varying function of μ_ν. The optimal per-site mutation probability then follows as

$$\mu^*_\nu = \frac{1}{n\sigma_\nu(\tau_{is} - \text{const}/\delta)} \approx \frac{1}{n\sigma_\nu\tau_{is}}. \qquad (10)$$

Figure 2 shows a comparison between the optimal mutation rate as given by the approximation (10), and the exact solution obtained numerically from (8). Despite the many approximations that have entered the derivation of (10), the analytic approximation is in good agreement with the numerical results. Improvements to the analytic approximation are possible if we neglect fewer of the higher order terms. [A significant improvement for small δ can be obtained if instead of completely neglecting the logarithmic term, we replace it with a constant (e.g., $\ln \mu_\nu \approx -7$ for μ_ν between about 10^{-4} and 10^{-2}.)]

Let us now rewrite (10) in terms of the optimal *genomic* mutation rate:

$$\mu^{G^*}_\nu := n\mu^*_\nu = \frac{1}{\sigma_\nu\tau_{is}}. \qquad (11)$$

This form suggests the following intuitive interpretation. The immune system adapts to a new virus strain within a

FIGURE 3

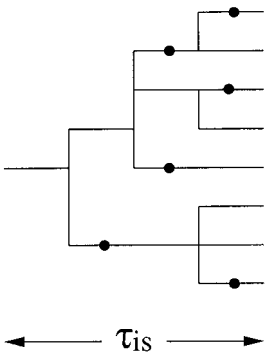

Regrowth from a single virus particle to a population size of eight, within the time-span τ_{is} (dots indicate mutations). The virus can best evade the immune system if almost every virion in the population at $t = \tau_{is}$ differs from the initial virion by one mutation.

time-span τ_{is}, whereas the virus replicates in a time-span $1/\sigma_\nu$. The ratio between these two time scales measures the duration of one generation of the virus in units of the response time of the immune system. Hence, Eq. (11) implies that the virus can optimally evade the immune system if the virus suffers on average *one* mutation per genome within the time the immune system needs to adapt to a new strain (Figure 3). This condition guarantees that a maximal number of virions have mutated away from the epitope to populate its first error class, *precisely* at that point in time when the immune system has adapted to attack the new viral quasispecies. A similar result has been obtained by Kimura who found that the optimal mutation rate at a locus is equal to the substitution rate needed at that locus to keep up with the changing environment [35].

If a viral quasispecies optimizes its mutation rate according to Eq. (11), we expect to see this reflected in a relation between the mutation rate and genome size, such that their product is constant (given a particular generation time $1/\sigma_\nu$). Optimization of genomic mutation rate can take place via an optimization of sequence length, given any particular per-site mutation rate. Table 1 shows that the genomic mutation rate μ_ν^G only slightly varies within the class of RNA viruses, which presumably have a similar generation time. This is well in agreement with the prediction (11).

Given the adaptation time of the immune system τ_{is} and the generation time $1/\sigma_\nu$, we can test the prediction of Eq. (11) more specifically. The adaptation time τ_{is} is the time necessary for the immune system to develop a specific answer to an antigen. For most systems, this can be estimated to take between 7 and 14 days [39]. The generation times of viral species of course vary, but data from HIV-1 is available. Table 2 shows that the optimal genomic mutation rate as predicted by formula (11) is well within the range of

TABLE 1

Genomic Length n and Spontaneous Mutation Rates per Base Pair and Replication μ_ν for RNA-based Viruses that Compete with Advanced Immune Systems as well as Genomic Mutation Rate, $\mu_\nu^G = n\mu_\nu$. Note that This Product is an Approximation for $\mu_\nu^G = 1 - (1 - \mu_\nu)^n$ for $n\mu_\nu < 1$

Organism	n	μ_ν	$\mu_\nu^G = n\mu_\nu$
Lytic RNA-based viruses [37]			
Poliovirus	7.4×10^3	1.1×10^{-4}	0.81
Influenza A virus	13.6×10^3	$>7.3 \times 10^{-5}$	0.99
RNA-based retroviruses [36,37]			
Spleen necrosis virus	7.8×10^3	2.0×10^{-5}	0.16
Molony murine leukemia virus	8.4×10^3	$>3.5 \times 10^{-6}$	0.029
Rous sarcoma virus	9.3×10^3	4.6×10^{-5}	0.43
HIV-1	9.2×10^3	2.4×10^{-5}	0.22

Data are reproduced from [36–38].

the experimentally determined rate. This suggests that HIV-1 has adapted its mutation rate to optimally escape the immune system as well as the error catastrophe.

4. SUMMARY

The dynamics of co-evolution between virus and immune system can be studied within the framework of molecular evolution in time-dependent fitness landscapes, in which a constantly changing, polymorphic, viral population competes with an immune system adapting to keep track of the viral changes. Such an analysis [34] reveals an optimal mutation rate for the immune system (so as to constrain the range of mutation rates within which the virus is stable) that appears to be compatible with available data. The same formalism can be used to determine the optimal *viral* mutation rate, by maximizing the speed of adaptation while minimizing information loss due to mutations. It follows that the optimal viral mutation rate is reached if a sequence undergoes on average *one* mutation within the time it takes for the immune system to

TABLE 2

Comparison of the Genomic Mutation Rate μ_ν^G of HIV-1 with the Theoretical Estimate $(\sigma_\nu \tau_{is})^{-1}$ from Formula (11)

	$\sigma_\nu[d^{-1}]$	$\tau_{is}[d]$	$(\sigma_\nu \tau_{is})^{-1}$	μ_ν^G
HIV-1	$0.4 \cdots 3.5$	$7 \cdots 14$	$0.02 \cdots 0.36$	0.22

Data are reproduced from [40, 41].

adapt to the viral genomic signature, thus barely staying ahead of the immune system. Such optimal mutation rates are compatible with experimentally determined ones and suggest that the constancy of genomic mutation rates within viral classes (while sequence length and per-site mutation rates vary over many orders of magnitude) can be explained by selection favoring viral strains at or near the optimal rate.

ACKNOWLEDGMENTS

This research was supported in part by the National Science Foundation under Contract No. DEB-9981397. Part of this work was carried out at the Jet Propulsion Laboratory under a contract with the National Aeronautics and Space Administration. Finally, C. Kamp thanks the Stiftung der Deutschen Wirtschaft for financial support.

REFERENCES

1. Eigen, M. Selforganization of matter and the evolution of biological macromolecules. Naturwissenschaften 1971, 58, 465–523.
2. Eigen, M.; Schuster, P. The hypercycle—a principle of natural self-organization. Springer-Verlag, Berlin, 1979.
3. Schuster, P.; Sigmund, K. Replicator dynamics. J Theoret Biol 1983, 100, 533–538.
4. Demetrius, L. Statistical mechanics and population biology. J Stat Phys 1983, 30, 709–753.
5. Demetrius, L.; Schuster, P.; Sigmund, K. Polynucleotide evolution and branching processes. Bull Math Biol 1985, 47, 239–262.
6. Schuster, P. Dynamics of molecular evolution. Physica D 1986, 22, 100–119.
7. Leuthäusser, I. An exact correspondence between Eigen's evolution model and a two-dimensional Ising system. J Chem Phys 1986, 84, 1884–1885.
8. Leuthäusser, I. Statistical mechanics of Eigen's evolution model. J Stat Phys 1987, 48, 343–360.
9. Schuster, P.; Swetina, J. Stationary mutant distribution and evolutionary optimization. Bull Math Biol 1988, 50, 635–660.
10. Nowak, M.; Schuster, P. Error thresholds of replication in finite populations, mutation frequencies and the onset of Muller's ratchet. J Theoret Biol 1989, 137, 375–395.
11. Tarazona, P. Error thresholds for molecular quasispecies as phase transitions: from simple landscapes to spin-glass models. Phys Rev A 1992, 45, 6038–6050.
12. Bonhoeffer, S.; Stadler, P.F. Error thresholds on correlated fitness landscapes. J Theoret Biol 1993, 164, 359–372.
13. Pastor-Satorras, R.; Sole, R.V. Field theory for a reaction-diffusion model of quasispecies dynamics. Phys Rev E 2001, 051909.
14. Domingo, E.; Biebricher, C.K.; Eigen, M.; Holland, J.J. Quasispecies and RNA virus evolution: principles and consequences. Landes Bioscience, Georgetown, TX, 2001.
15. Alves, D.; Fontanari, J.F. Error threshold in the evolution of diploid organisms. J Phys A Math Gen 1997, 30, 2601–2607.
16. Campos, P.R.A.; Fontanari, J.F. Finite-size scaling of the quasispecies model. Phys Rev E 1998, 58, 2664–2667.
17. Campos, P.R.A.; Fontanari, J. F. Finite-size scaling of the error threshold transition. J Phys A 1999, 32, L1–L7.
18. Altmeyer, S.; McCaskill, J.S. Error threshold for spatially resolved evolution in the quasispecies model. Phys Rev Lett 2001, 86, 5819–5822.
19. Hermisson, J.; Redner, O.; Wagner, H.; Baake, E. Mutation-selection balance: Ancestry load, and maximum principle. Theor Popul Biol 2002, 62, 9–46.
20. Loeb, L.A.; Essigmann, J.M.; Kazazi, F.; Zhang, J.; Rose, K.D.; Mullins, J.I. Lethal mutagenesis of HIV with mutagenic nucleoside analogs. Proc Natl Acad Sci USA 1999, 96, 1492–1497.
21. Crotty, S.; Cameron, C.E.; Andino, R. RNA virus error catastrophe: direct molecular test by using ribavirin. Proc Natl Acad Sci USA 2001, 98, 6895–6900.
22. van Nimwegen, E.; Crutchfield, J.P.; Huynen, M. Neutral evolution of mutational robustness. Proc Natl Acad Sci USA 1999, 96, 9716–9720.
23. Wilke, C.O.; Wang, L.J.; Ofria, C.; Lenski, R.E.; Adami, C. Evolution of digital organisms at high mutation rates leads to survival of the flattest. Nature 2001, 412, 331–333.
24. Wilke, C.O. Selection for fitness versus selection for robustness in RNA secondary structure folding. Evolution 2001, 55, 2412–2420.
25. Nilsson, M.; Snoad, N. Error thresholds for quasispecies in dynamic fitness landscapes. Phys Rev Lett 2000, 84, 191–194.
26. Wilke, C.O.; Ronnewinkel, C.; Martinetz, T. Dynamic fitness landscapes in molecular evolution. Phys Rep 2001, 349, 395–446.
27. de Visser, J.A.G.M. The fate of microbial mutators. Microbiology 2002, 148, 1247–1252.
28. LeClerc, J.E.; Li, B.; Payne, W.L.; Cebula, T.A. High mutation frequencies among *Escherichia coli* and *Salmonella* pathogens. Science 1996, 274, 1208–1211.
29. Sniegowski, P.D.; Gerrish, P.; Lenski, R.E. Evolution of high mutation rates in experimental populations of *E. coli.* Nature 1997, 387, 703–705.
30. Giraud, A.; Matic, I.; Tenaillon, O.; Clara, A.; Radman, M.; Fons, M.; Taddei, F. Costs and benefits of high mutation rates: adaptive evolution of bacteria in the mouse gut. Science 2001, 291, 2606–2608.
31. Harris, R.S.; Kong, Q.; Maizels, N. Somatic hypermutation and the three R's: repair, replication and recombination. Mutat Res 1999, 436, 157–178.
32. Ganeshan, S.; Dickover, R.E.; Korber, B.T.M.; Bryson, Y.J.; Wolinsky, S.M. Human immunodeficiency virus type 1 genetic evolution in children with different rates of development of disease. J Virol 1997, 71, 663–677.
33. Allen, T.M.; O'Connor, D.H.; Jing, P.; Dzuris, J.L.; Mothe, B.R.; Vogel, T.U.; Dunphy, E.; Liebl, M.E.; Emerson, C.; Wilson, N.; Kunstmann, K.J.; Wang, X.; Allison, D.B.; Hughes, A.L.; Desrosiers, R.C.; Altman, J.D.; Wolinsky, S.M.; Sette, A.; Watkins, D. Tat-specific cytotoxic T lymphocytes select for SIV escape variants during resolution of primary viraemia. Nature 2000, 407, 386–390.
34. Kamp, C.; S. Bornholdt, Co-evolution of quasispecies: B-cell mutation rates maximize viral error catastrophes. Phys Rev Lett 2002, 88, DOI068104.
35. Kimura, M. On the evolutionary adjustment of spontaneous mutation rates. Genet Res 1967, 9, 23–34.
36. Drake, J.W.; Charlesworth, B.; Charlesworth, D.; Crow, J.F. Rates of spontaneous mutation. Genetics 1998, 148, 1667–1686.
37. Drake, J.W. Rates of spontaneous mutation among RNA viruses. Proc Natl Acad Sci USA 1993, 90, 4171–4175.
38. Drake, J.W.; Holland, J.J. Mutation rates among RNA viruses. Proc Natl Acad Sci USA 1999, 96, 13910–13913.
39. Roitt, I. Essential Immunology; Blackwell Scientific Publications, Oxford, 1994.
40. Little, S.J.; McLean, A.R.; Spina, C.A.; Richman, D.D.; Havlir, D.V. Viral dynamics of acute HIV-1 infection. J Exp Med 1999, 190, 841–850.
41. Perelson, A.S.; Neumann, A.U.; Markowitz, M.; Leonard, J.M.; Ho, D.D. HIV-1 dynamics in vivo: virion clearance rate, infected cell life-span, and viral generation time. Science 1996, 271, 1582–1586.